

# Photocatalytic kinetics of phenol and its derivatives over UV irradiated TiO<sub>2</sub>

Dingwang Chen, Ajay K. Ray\*

*Department of Chemical and Environmental Engineering, National University of Singapore, 10 Kent Ridge Crescent,  
Singapore 119260, Singapore*

Received 8 February 1999; received in revised form 11 June 1999; accepted 11 June 1999

## Abstract

In recent years, photocatalytic degradation mediated by illuminated TiO<sub>2</sub> has received considerable attention as an alternative for treating polluted water. In the present study, a new two-phase swirl-flow monolithic-type reactor was used to study the kinetics of heterogeneous photocatalytic processes. Photocatalytic degradation of phenol, 4-chlorophenol (4-CP) and 4-nitrophenol (4-NP) both in aqueous suspensions and over immobilized Degussa P25 TiO<sub>2</sub> has been studied in laboratory scale. Experiments were conducted to investigate the effects of parameters such as catalyst dosage, pollutant concentration, temperature, partial pressure of oxygen, UV light intensity, catalyst-layer thickness, circulation flowrate and catalyst annealing temperature. Simple model for predicting the optimal catalyst dosage in aqueous suspensions for different photo-systems was proposed. Pseudo first-order kinetics with respect to all the parent compounds was observed. Experimental data obtained under different conditions were fitted with kinetic equation to describe the dependency of degradation rate as a function of the above mentioned parameters. Consequently, kinetic parameters were experimentally determined. Adsorptive properties of all the organics were also experimentally measured and fitted with Langmuir equation. The extreme low surface coverage of the organics on the catalyst may be one of the main factors that result in the low efficiency of the photocatalytic process. Besides, mass transfer of organics and oxygen in the photocatalytic process has also been discussed in detail. ©1999 Elsevier Science B.V. All rights reserved.

*Keywords:* Photocatalytic oxidation; Photodegradation; TiO<sub>2</sub> catalyst; Kinetic study; Phenol

## 1. Introduction

The efficient treatment of industrial wastewaters and contaminated drinking water sources has become of immediate importance in a world that is facing with ever increasing population and decreasing energy resources. An ideal waste treatment process will completely mineralize all the toxic species present in the

waste stream without leaving behind any hazardous residues. It should also be cost-effective. At the current state of development, none of the treatment technologies approach this ideal situation. Air stripping, which is commonly employed for the removal of volatile organic contaminants in wastewater, just transfers the pollutants from water phase to air phase rather than destroying them. Thus, most air-stripping processes currently require subsequent treatment of the off-gas. Granular activated carbon (GAC) adsorption is the other commercialized process for water purification.

\* Corresponding author. Tel.: +65-874-8049; fax: +65-779-1936  
E-mail address: cheakr@nus.edu.sg (A.K. Ray)

However, the spent carbon, on which pollutants are adsorbed, is a new waste that needs to be disposed of. Biological degradation of municipal wastes has been practiced, but similar biotreatment of industrial wastes are still not common because some toxic organics may kill the active micro-organisms. Heterogeneous photocatalysis is one of the advanced oxidation processes (AOPs) that has proven to be a promising method for the elimination of toxic and bio-resistant organic and inorganic compounds from wastewater by transforming them into innocuous species [1–3].

Many examples of complete photo-oxidation of organic compounds have been reported. Matthews studied the photocatalytic degradation of 22 organics both in TiO<sub>2</sub> aqueous suspensions [4,5] and over immobilized TiO<sub>2</sub> thin films [6,7]. Pruden and Ollis [8] carried out the photomineralization of halogenated organic pollutants in TiO<sub>2</sub> suspensions. Pelizzetti et al. [9] investigated the photo-degradation of herbicides and surfactants. In most of the above studies, Langmuir–Hinshelwood model was used to describe the degradation rate expressions in terms of the disappearance of compounds or the formation of CO<sub>2</sub>. It has been demonstrated that catalyst dosage, initial concentration of pollutants, UV light intensity, dissolved oxygen, temperature, circulating flowrate and pH of the solution are the main parameters affecting the degradation rate. It is well known that kinetic modelling of the photocatalytic process is essential to any practical applications. Several kinetic models have been published in literature [7,10–13], but none of them could completely account for all possible variables affecting the degradation rate. Almost all these studies investigated the effects of various parameters on the initial degradation rate rather than the degradation rate during the whole photomineralization process. The degradation kinetic rate expressions have so far focused on the initial disappearance rate of organic compounds [12] or the initial formation rate of CO<sub>2</sub>[7,11]. Moreover, initial rate data are tedious to obtain and prone to variation, thereby reducing the reliability of the results. Optimal TiO<sub>2</sub> catalyst dosage in aqueous suspensions reported has a wide range from 0.15 to 8 g/l for different photosystems, and reactor configurations, and no quantitative explanation was reported. Most commonly proposed mechanism is usually based on the reaction between the adsorbed species. Chen et al. [14] and Cunning-

ham and Al-Sayyed [15] investigated the adsorption properties of dichloroethane and substituted benzoic acids, respectively over P25 TiO<sub>2</sub>. However, to our knowledge, no adsorptive results of phenol and its derivatives have been published. In this paper, the photodegradation of phenol, 4-chlorophenol (4-CP) and 4-nitrophenol (4-NP) mediated by illuminated P25 TiO<sub>2</sub> in aqueous suspensions and over immobilized catalyst film has been investigated systematically. Experiments were conducted to study the effects of operational parameters on the degradation rate or catalyst activity. A degradation kinetic expression, which can be used in the design of large-scale photocatalytic reactor and subsequently, optimization of experimental conditions, was proposed, which can satisfactorily predict the photodegradation behaviour under different conditions. A simple model that can foretell the optimal catalyst dosage for different systems was proposed and has been verified for the photodegradation of phenol, 4-CP and 4-NP. In order to elucidate the process, the adsorptive experiments of above compounds on TiO<sub>2</sub> have also been studied. Moreover, the mass transfer of organics and O<sub>2</sub>, which is another factor that must be taken into consideration in photocatalytic process, particularly for catalyst immobilized systems, has also been discussed quantitatively.

## 2. Experimental details

### 2.1. Materials

Degussa P25 catalyst provided by Degussa Company was used throughout this work without further modification. Its main physical data are as follows: BET surface area  $55 \pm 15 \text{ m}^2/\text{g}$ , average primary particle size around 30 nm, purity above 97% and with 80:20 anatase to rutile. All other chemicals, 4-NP (98+%) and salicylic acid (99.7%) from BDH chemicals, phenol (99.5+%), hydrochloric acid (37%) and nitric acid (65% by weight) from Merck chemicals, 4-CP (99+%) from Fluka chemicals, acetonitrile (for HPLC) from Fisher, sodium hydroxide (98+%) from Baker chemicals, were used as received. Water used to make up solutions in this work was Milli-Q water.

## 2.2. Apparatus and analyses

The semi-batch photoreactor consists of two circular glass plates that are placed between soft padding housed within stainless steel and aluminium casings. The TiO<sub>2</sub> aqueous solution, which was circulated by a peristaltic pump, was introduced tangentially between the two glass plates, and exited from the center of the top plate. Residence time distribution of this type of reactor indicated that the tangential introduction of liquid made the reaction solution well mixed in the reactor [16]. The lamp (Philips HPR 125W high-pressure mercury vapour) was placed about 10 cm underneath the bottom glass plate on a holder that could be moved to create a different angle of incidence of light on the bottom glass plate. Primary radiation of this lamp is emitted at 365 nm. The lamp and reactor were placed inside a wooden box painted black so that no stray light can enter the reactor. The lamp was constantly cooled by compressed air to keep the temperature down and protect the lamp from overheating. Provision was made for placement of several metal screens of different mesh size between the lamp and bottom glass plate to vary the light intensity in the range of 1.5–24 mW/cm<sup>2</sup>. The detailed configuration of the photoreactor is described elsewhere [16].

A Shimadzu TOC-5000A analyzer with an ASI-5000 autosampler was used to analyze the TOC in samples. Analyses of 4-NP, 4-CP and phenol were carried out by using a Shimadzu UV 3101 PC spectrophotometer and a HPLC (Perkin Elmer). Aliquots of 20 ml were injected onto a reverse-phase C-18 column (Chrompack), and eluted with the mixture of acetonitrile (60%) and ultrapure water (40%) at the total flowrate of 1.5 ml/min. Absorbance at 225 and 319 nm was used to measure the concentration of above compounds by a UV/VIS detector (Perkin Elmer). All water samples were filtered by Millex-HA filter (Millipore, 0.45 μm) before analyses. The Cyberscan 2000 pH meter and Orion 720A ion meter measured the pH value and chloride ion concentrations of the reaction solution, respectively.

Adsorption experiments were carried out using 50 ml of various samples with different concentrations in which 1 g TiO<sub>2</sub> was added in. Suspensions were placed into 100 ml conical flasks and shaken by a laboratory shaker at 300 min<sup>-1</sup> for 24 h at room temperature. After 12 h' stationary settlement, clear

samples were obtained by filtering the solutions using Millipore filter (0.45 μm). In order to have a precise concentration result, samples were doubly measured by UV spectrophotometer and HPLC.

## 2.3. Preparation of the immobilized catalyst

The support used in this study was 3.2 mm thick circular Pyrex glass plate because it can cut off the UV light below 300 nm thereby eliminating the direct photolysis of the organic compounds studied. In order to have a good adhesion for the catalyst to the glass surface, the coated side was roughened by sand blasting. The glass plate was cleaned with acid followed by alkaline solution overnight to remove impurities, washed with Millipore Milli-Q water, and finally dried at 393 K for 2 h. The TiO<sub>2</sub> suspension (5 wt.%) was prepared in an ultrasonic cleaner bath for 1 h to obtain a milky solution that can be kept stable for weeks. The substrate was then coated with catalyst by dipping it into the suspension and pulling it out of slowly by the dip-coating technique. The catalyst coating was dried at 393 K for half-hour. Above procedure was repeated up to 15 times depending on the desired mass of coated catalyst. Finally, the coated glass plate was calcined in a furnace by raising the temperature gradually at a rate of 5 K/min to final temperature of 423–873 K, for different glass plates, and held there for 3 h and cooled down using the same ramping rate until it reached the room temperature. Gradual heating and cooling is necessary as otherwise the catalyst film might crack. After that the coated catalyst film was brushed tenderly and flushed with water to remove the loosely bound catalyst particles. The total mass of catalyst deposited per unit area (or thickness) was determined by weighing the glass plate before and after the catalyst coating.

## 3. Results and discussion

### 3.1. Photodegradation of organics

In this paper, degradation of 4-CP, 4-NP and phenol over illuminated P25 TiO<sub>2</sub> was investigated, and the results demonstrated that all compounds could be completely degraded into CO<sub>2</sub>, water and corresponding mineral acids. Fig. 1 illustrates the degradation course

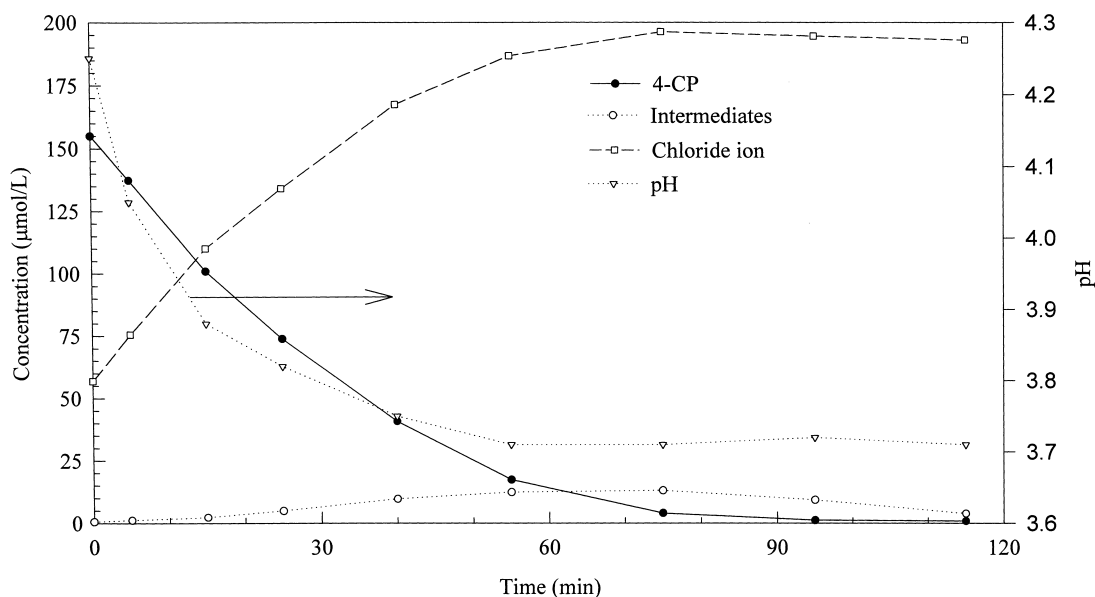


Fig. 1. Typical diagram of the degradation of 4-CP in P25 TiO<sub>2</sub> suspensions. (Experimental conditions:  $I=22\text{ mW/cm}^2$ ,  $C_0=0.16\text{ mM}$ ,  $(\text{TiO}_2)=2\text{ g/l}$ , O<sub>2</sub> saturated).

of 4-CP, formation and subsequent degradation of intermediates, chloride ion concentration and pH variation during the photocatalyzed reaction. The decrease of pH value in solution resulted from the formation of HCl during the degradation, which was reflected by the increase of the chloride ion concentration. In literature [17] up to six intermediates have been detected during the degradation of 4-CP in TiO<sub>2</sub> aqueous slurry, and all of that could be degraded further to final products CO<sub>2</sub> and HCl. Under the experimental conditions in the present work, the total concentration of intermediates measured during the reaction was quite low, therefore no effort has been made to identify them. The total concentration of intermediates was determined as the difference between the concentrations of TOC and 4-CP under the assumption that all formed intermediates consist of six carbon atoms. Sample concentrations of TOC and 4-CP were measured by the TOC analyzer and HPLC respectively. Total chloride ion balance was carried out in the reaction system by measuring the concentration of 4-CP, intermediates and chloride ion in solution for each sample drawn. The average total chloride ion concentration measured for nine samples with 212 mM initial chloride ion was  $205.2 \pm 7.06\text{ mM}$ , without consider-

ing the chloride ion present in intermediates. Average total chloride ion concentration of  $211.5 \pm 6.2\text{ mM}$  was obtained when it was assumed that each mole intermediates contains 1 mol chloride ion. Above results indicated that no significant loss of chloride ion was observed due to the photo-induced adsorption of 4-CP onto the TiO<sub>2</sub> particles and/or formation of high volatility intermediates. The slight decrease of total chloride ion concentration with reaction time was due to the adsorption of chloride ion on the TiO<sub>2</sub> catalyst. It should be noted that the initial concentration of chloride ion concentration in Fig. 1 comes from the trace content of HCl present in the commercial P25 TiO<sub>2</sub>, which was reported in the manufacturer's document.

The gradual disappearance of 4-CP was monitored during the photocatalytic reaction by recording the UV spectra of samples in the 200–350 nm range. Typical spectra are shown in Fig. 2. The characteristic absorption of 4-CP almost disappeared after 100 min of irradiation under the experimental conditions. No peak for intermediates was detected due to the low concentration of intermediates.

It should be pointed out that there are two types of photocatalytic degradation for the coloured compound 4-NP, i.e. *direct* photocatalysis and *sensitized* photo-

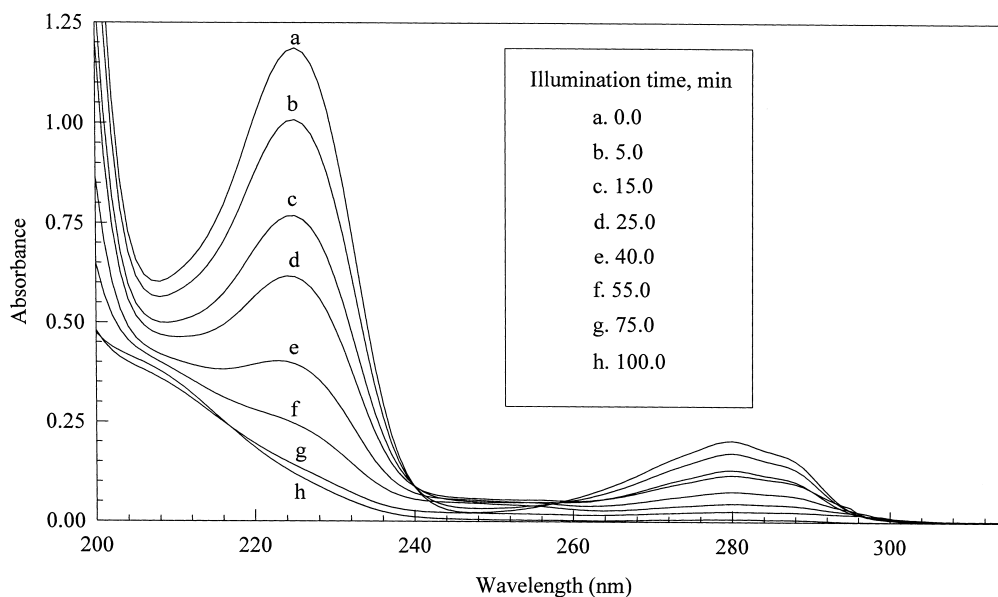


Fig. 2. UV spectrum profiles during the degradation of 4-CP in P25 TiO<sub>2</sub> suspensions. (Experimental conditions:  $I=20.5 \text{ mW/cm}^2$ ,  $C_0=0.16 \text{ mM}$ ,  $(\text{TiO}_2)=2 \text{ g/l}$ , O<sub>2</sub> saturated).

catalysis. The *direct* photocatalysis is the one discussed in this paper. In *sensitized* photocatalysis, the adsorbed coloured compound is promoted to an excited state by the input of *visible* radiation. The excited 4-NP can then inject an electron into the conduction band of the semiconductor and become oxidized to a cation radical. Hence, this process does not involve charge separation in photocatalyst and formation of hydroxyl radical, which are essential in *direct* photocatalysis. Recently, Dieckmann and Gray [18] compared these two types of photocatalytic degradation of 4-NP in Degussa P25 suspensions. They reported that the pseudo-first order rate constants for *direct* and *sensitized* photocatalysis were  $2.02$  and  $0.122 \text{ h}^{-1}$ , respectively. Obviously, *direct* photocatalysis is much more efficient than *sensitized* photocatalysis. Meanwhile, one should note that sensitized photocatalysis for 4-NP degradation occurs mainly in alkaline solution. In alkaline solution, 4-NP ( $\text{p}K_{\text{a}}=7.15$ ) is predominantly present in the deprotonated form, which strongly absorbs visible light ( $\lambda_{\text{max}}=399 \text{ nm}$ ;  $\epsilon=6.99 \times 10^3 \text{ l/mol/cm}$ ), while the protonated form weakly absorbs visible light ( $\lambda_{\text{max}}=319 \text{ nm}$ , extinction coefficient  $\epsilon=6.99 \times 10^3 \text{ l/mol/cm}$ ) [18]. However, in our experimental study for the degradation of 4-NP solution pH was around 4. The primary emis-

sion of our UV lamp was at  $365 \text{ nm}$  and no radiation at wavelength of  $319 \text{ nm}$  was generated. Therefore, in our experimental studies photocatalytic degradation rate of 4-NP resulted from *sensitized* photocatalysis was negligible.

### 3.2. Catalyst dosage

In slurry photocatalytic processes, catalyst dosage is an important parameter that has been extensively studied. Table 1 lists the research results reported in literature. Obviously, the optimal catalyst dosage reported was in a wide range from  $0.15$  to  $8 \text{ g/l}$  for different photocatalyzed systems and photoreactors. Even for the same catalyst (Degussa P25), a big difference in optimal catalyst dosage (from  $0.15$  to  $2.5 \text{ g/l}$ ) was reported. Till now no general conclusion has been made.

Fig. 3 is the schematic diagram of the UV light distribution in the photoreactor used in this study. Because the photodegradation takes place on the surface of catalyst, the degradation rate in a differential volume is proportional to the illuminated catalyst surface area and can be written as:

$$dr_i = k_1 f(C_i) I_z^\beta A_{\text{cat}} dz \quad (1)$$

Table 1  
List of optimal catalyst dosage reported in literature

Pollutant(s)	Catalyst	Optimal dosage (g/l)	Reference
2- and 3-CP	Degussa P25 TiO <sub>2</sub>	2.5	[22]
4-CP	Degussa P25 TiO <sub>2</sub>	2.0	[20]
Nitrophenols	TiO <sub>2</sub> from BDH	1.0	[23]
Methyl orange	Anatase TiO <sub>2</sub> from Merck Co.	8.0	[10]
4-CP	Degussa P25 TiO <sub>2</sub>	0.5	[17]
Carbetamide	Degussa P25 TiO <sub>2</sub>	0.2	[21]
Methylene blue	Degussa P25 TiO <sub>2</sub>	0.15	[24]
Dimethylphenols	Degussa P25 TiO <sub>2</sub>	1.0	[25]
Malonic acid	Degussa P25 TiO <sub>2</sub>	0.8	[12]
2-CP	TiO <sub>2</sub> from CERAC Inc.	2.0	[19]
Cyanides	Home prepared TiO <sub>2</sub>	2.0	[26]

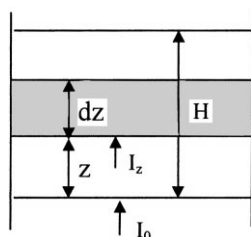


Fig. 3. Schematic diagram of light absorption in the photoreactor.

and

$$I_z = I_0 \exp(-\varepsilon C_{\text{cat}} z) \quad (2)$$

where  $C_i$  is the concentration of pollutant  $i$  in the bulk solution,  $I_0$  the incident light intensity,  $A$  the illuminated area of the reactor window,  $C_{\text{cat}}$  the catalyst concentration,  $\varepsilon$  the light absorption coefficient of catalyst in suspensions and  $k_1$  a proportional constant. Substituting Eq. (2) into Eq. (1) then integrating Eq. (1) for the reactor depth  $H$  at a given  $C_i$  and  $I_0$  yields:

$$r_i = K [1 - \exp(-\varepsilon \beta C_{\text{cat}} H)] \quad (3)$$

where

$$K = \frac{k_1 A f(C_i) I_0^\beta}{\varepsilon \beta} \quad (4)$$

The  $\beta$  values listed in Table 2, Column 4 for different photocatalyzed systems were determined experimentally by carrying out experiments at different light intensities. Detailed experimental procedures were reported in our previous paper [27]. Eq. (3) can well correlate the results depicted in Fig. 4 for all the three

components in the photocatalyzed system. The solid lines were calculated using Eq. (3) with the  $\varepsilon$  values listed in Column 7 of Table 2. The  $\varepsilon$  values for the three systems were obtained from Eq. (3) by least square fitting of the experimental data and the values obtained were very close to each other. The result supports the reliability of the above simple model because the  $\varepsilon$  value should be same for the same catalyst in dilute solutions of different organics.

Eq. (3) can also successfully explain the dependence of degradation rate on the TiO<sub>2</sub> dosage at different light intensities. Degradation rate is usually proportional to  $I^{0.5}$  and  $I^{1.0}$  at high and low intensities, respectively. Thus, according to Eq. (3) the optimal catalyst dosage at high light intensity is higher than that at low light intensity. The result reported in this paper is in accord with those obtained by Okamoto et al. [28], Ku et al. [19] and Crittenden et al. [29]. They reported that the optimal catalyst dosage increased slightly with the increasing light intensity. In order to further verify Eq. (3), experiments have been carried out for the degradation of the three model compounds in four similar reactors having different depths from 15 to 61 mm. The results show that the degradation rate scarcely changed with the increase of the reactor depth. This indicated that the optical penetration length was less than 15 mm at the experimental TiO<sub>2</sub> dosage and light intensity. Eq. (3) can be applied to predict the optimal catalyst dosage for different reactor geometry or different solution thickness in the light penetration direction. The optimal catalyst dosage or effective optical penetration length under given conditions is very important to the design of a slurry reactor for effective use of the reactor space and

Table 2  
Kinetic parameters for 4-NP, 4-CP and phenol in Eq. (7) and light absorption coefficient of P25 TiO<sub>2</sub>

Pollutant	$k_0$ (mol/m <sup>2</sup> /s)	$E$ (kJ/mol)	$\beta$	$K_{O_2}$ (atm <sup>-1</sup> )	$K_s$ (mM <sup>-1</sup> )	$\epsilon$ (l/g/cm)
4-NP	$1.34 \times 10^{-5}$	7.42	0.84	9.98	10.43	1.58
4-CP	$3.03 \times 10^{-4}$	13.72	0.72	17.64	6.24	1.71
Phenol	$1.19 \times 10^{-4}$	11.80	0.82	12.71	4.26	1.76

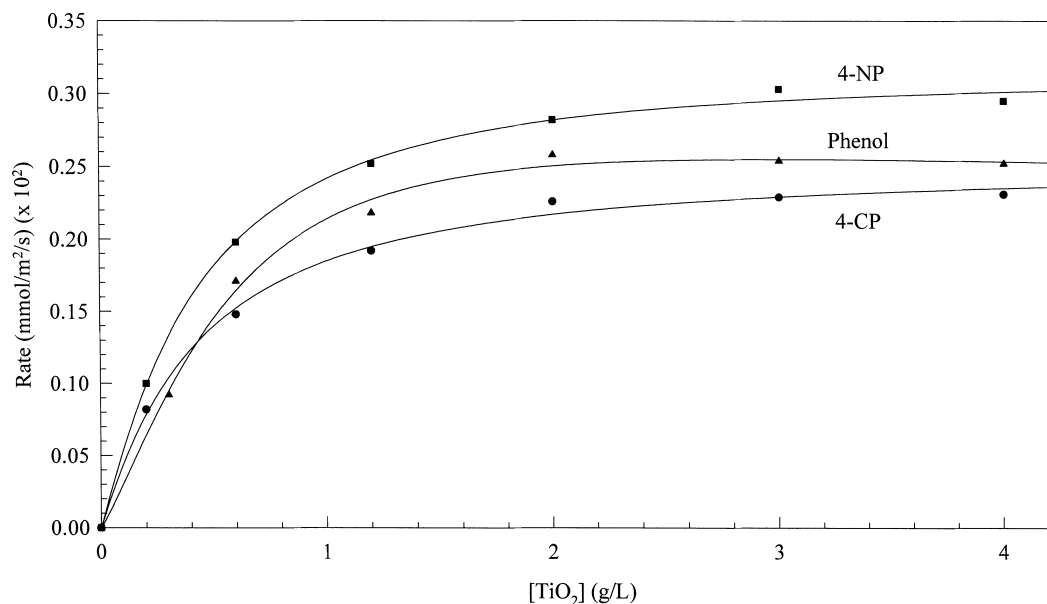


Fig. 4. Effect of catalyst dosage on the degradation rate of 4-NP, 4-CP and phenol. (Experimental conditions: O<sub>2</sub> saturated, pH natural; Phenol:  $I = 17.5$  mW/cm<sup>2</sup>;  $C_0 = 0.20$  mM; 4-NP:  $I = 18.3$  mW/cm<sup>2</sup>;  $C_0 = 0.144$  mM; 4-CP:  $I = 13.0$  mW/cm<sup>2</sup>;  $C_0 = 0.16$  mM).

catalyst. If the thickness of reaction solution is much larger than the optical penetration length at any given illumination intensity and catalyst concentration, the photoreactor will be under-utilized. Theoretically, increasing catalyst loading above the optimal value becomes inconsequential as all available light will already be utilized. However, considering other effects that are different from those related to radiation absorption, the catalyst concentration employed in practical applications is usually higher than the predicted optimal value. Therefore, Eq. (3) predicts the optimal catalyst dosage, and should be used as a basis in the photocatalytic reactor design.

For TiO<sub>2</sub> immobilized system, there also exists an optimal thickness of the catalyst film. Fig. 5 represents the influence of catalyst thickness on the observed rate constant of 4-NP for TiO<sub>2</sub> deposited system. The interfacial area is proportional to the thickness

of catalyst as the film is porous. Thus, thick film favors catalytic oxidation. On the other hand, the internal mass transfer resistance for both organic species and photo-generated electron/hole will increase with the increasing film thickness. This raises the recombination possibility of the electron/hole pair, and as a consequence it reduces the degradation performance. The optimal catalyst loading for TiO<sub>2</sub> immobilized system found experimentally in this study was around 0.8 mg/cm<sup>2</sup>. Influence of the catalyst thickness on the degradation rate can be described by [30]:

$$\frac{r_s}{r_{s, \max}} = \frac{\alpha\beta}{(k_f/D_e) - \alpha\beta} [\exp(-\alpha\beta h) - \exp(-k_f/D_e h)] \quad (5)$$

and optimum catalyst thickness is given by:

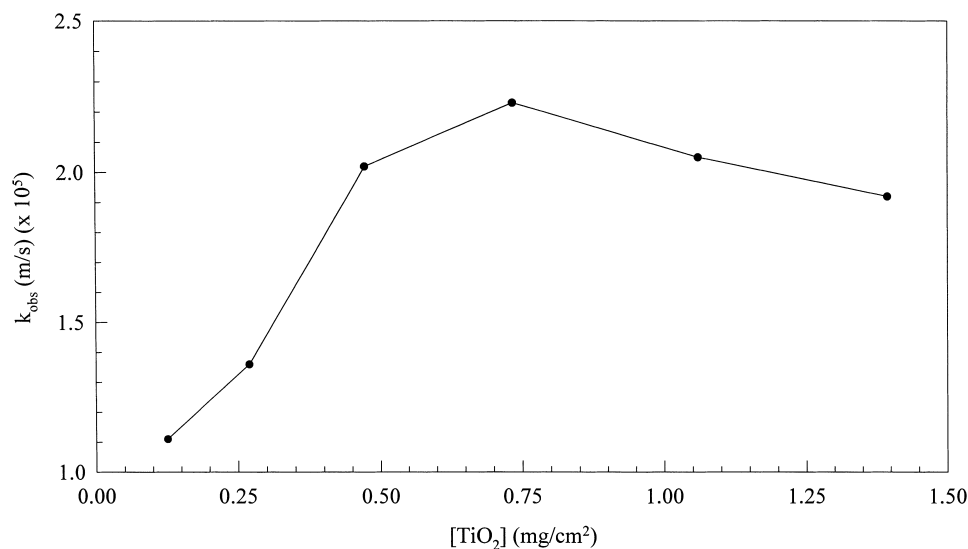


Fig. 5. Dependence of rate constant of 4-NP on the catalyst loading in TiO<sub>2</sub> immobilized system. (Experimental conditions:  $I = 16.2 \text{ mW/cm}^2$ ;  $C_0 = 1.0 \text{ mM}$ ;  $T = 303 \text{ K}$ ,  $Q = 425 \text{ ml/min}$ ; O<sub>2</sub> saturated, pH natural).

$$h_{\text{opt}} = \frac{\ln(\alpha\beta D_e/k_f)}{\alpha\beta - (k_f/D_e)} \quad (6)$$

where  $\alpha$  is light adsorption coefficient of catalyst film,  $D_e$  the effective diffusivity of pollutant in catalyst film and  $k_f$  the internal mass transfer resistance factor.

### 3.3. Degradation kinetics

Besides the catalyst dosage, effects of other kinetic factors on the photocatalytic degradation that were investigated in this work include initial concentration of pollutants, UV light intensity, dissolved oxygen concentration and temperature. Based on the derivation made in the earlier paper [27], the photocatalytic degradation kinetics for 4-NP, 4-CP and phenol have the following expression:

$$r_s = -\frac{dn_s}{Sdt} = k_0 \exp[-(E/RT)] I_a^\beta \frac{K_{O_2} p_{O_2}}{(1 + K_{O_2} p_{O_2})} \times \frac{K_s C_s}{1 + K_s C_{s0}} \quad (7)$$

In above equation, the photodegradation rate ( $\text{mol/m}^2\text{s}$ ) was defined as the mole ( $n_s$ ) reduction of pollutant converted per irradiated reactor window area ( $S$ ). All experiments were performed at natural pH value and at a constant TiO<sub>2</sub> dosage of 2 g/l, while other

parameters were varied as follows:  $T = 288\text{--}323 \text{ K}$ ;  $I_a = 1.5\text{--}24 \text{ mW/cm}^2$ ;  $C_{s0} = 0.07\text{--}0.9 \text{ mM}$ , and  $p_{O_2} = 0.05\text{--}1.0 \text{ atm}$ . In kinetic study of photocatalytic degradation, the equilibration time for adsorption of both organics and dissolved oxygen under dark conditions is an important variable, especially for the determination of the initial degradation rate. In this study, the solution in the reactor was illuminated only after the adsorption equilibrium was established. Kinetic parameters in Eq. (7) were determined by least square fitting of the above equation with the experimental data obtained under different conditions, and are listed in Table 2.

Unlike other advanced oxidation processes, which are based on the addition of chemical reagents, in photocatalysis the observed degradation rate of an organic substrate usually exhibits a saturation behavior. The denominator reflects this in the last term in Eq. (7). The observed degradation rate constant decreases with the increase of initial pollutant concentration. Other authors [10–13,22,23] reported similar results. However, the mechanism of this effect is still not clear. In this paper, we propose three factors that might be responsible for the saturation behaviour during the photocatalytic reaction.

Firstly, according to the principles of photocatalytic reaction, the main steps in the process occur on the



surface of the solid semiconductor photocatalyst [31], so the adsorption of organic compounds on the catalyst surface definitely affects the reaction and usually high adsorption capacity favours to the reaction. For most organic compounds adsorption capacity on TiO<sub>2</sub> catalyst can be well described by Langmuir equation. This has been confirmed in this study. This means that at high initial concentration all catalytic sites of the semiconductor catalyst surface are occupied. A further increase in pollutant concentration does not affect the actual catalyst surface concentration and therefore, this may result in the decrease of observed first order rate constant at higher initial concentration. Secondly, the generation and migration of the photogenerated electron-hole pair, and the reaction between photogenerated hole (or hydroxyl radical) and organic compounds are two processes that occur in series. Therefore, each step may become rate determining for the overall process. At low concentration the latter dominates the process and, therefore, the degradation rate increases linearly with the concentration. On the contrary, at high concentration the former will become the governing step and the degradation rate increases slowly with concentration, and even a constant degradation rate may be observed at higher concentration for a given illuminating light intensity. Gerischer and Heller [32] and Wang et al. [33] proposed substantial evidence indicating that the interfacial electron transfer process involving the reduction of oxygen was the rate-determining step in the TiO<sub>2</sub> sensitized photodegradation of organics. Lastly, intermediates generated during the photocatalytic process also affect the rate constant of their parent compounds. For example, two experimental runs with different initial concentrations  $C_1$  and  $C_2$  ( $C_1 > C_2$ ) are performed. When experiment starting with  $C_1$  decreases to  $C_2$ , some intermediates will be formed and subsequently will be adsorbed competitively on the solid catalyst surface. Whereas, for the other experimental run with the initial concentration  $C_2$ , no intermediates are present at the beginning. The presence of intermediates for the first run reduces the effective concentration of the parent compound on the catalyst surface thereby resulting in the decrease of the overall observed rate.

The overall process of photocatalytic degradation is usually not very temperature sensitive. The dependence of degradation rate on temperature is reflected by the low activation energy compared with the ordi-

nary thermal reactions. This is observed by the low activation energies obtained in this work for the three model compounds and the values are comparable with the reported values of 5–20 kJ/mol [27]. Therefore, the influence of temperature is quite weak. This is because of the low thermal energy ( $kT = 0.026$  eV at room temperature) that has almost no contribution to the activation of TiO<sub>2</sub> catalyst, which has a high bandgap energy (3.2 eV). Consequently, contrary to thermal reactions, there is no need to heat the system. This absence of heating is very attractive for photocatalytic processes carried out in aqueous media, especially for water purification, because there is no need to waste energy in heating water, which has a high heat capacity. On the other hand, these activation energies are quite close to that of a hydroxyl radical reaction [6], suggesting that the photodegradation of the above organics were governed by the hydroxyl radical reaction.

Presence of electron acceptor is necessary to remove the photo-generated electrons for continuation of the photocatalytic oxidation of organic compounds. Otherwise, the accumulated photons in the catalyst particle will recombine with holes, which are the initiators of the photocatalytic reaction. The commonly used electron acceptor is oxygen as it is easily available, soluble under most conditions and non-toxic to environment. Wang et al. [33] observed that the photocatalytic activity was nearly completely suppressed in the absence of oxygen and the steady-state concentration of oxygen has a profound effect on the rate of photocatalyzed decomposition of organic compounds. Alberici and Jardim [34] found that the decomposition of phenol non-aerated solutions containing TiO<sub>2</sub> was much slower compared with aerated ones. Sabate et al. [35] did not observe photocatalytic degradation of 3-chlorosalicylic acid when pure N<sub>2</sub> was bubbled through the solution. Hsiao et al. [36] found that the observed rate of disappearance of dichloro- and trichloromethane was much faster when the solution was well purged with oxygen. Sclafani et al. [37] found that the concentration decay of phenol was much faster when oxygen was bubbled through the solution containing anatase TiO<sub>2</sub> instead of He. In the present study, in order to evaluate the effects of the dissolved oxygen concentration on the rate of the photocatalytic reaction, a series of experiments were conducted in which the O<sub>2</sub>/N<sub>2</sub> ratio in the gas feed stream was varied while the total flowrate was kept constant. Since

Table 3  
Adsorption constant of dissolved oxygen on TiO<sub>2</sub> catalyst

Pollutant	Catalyst	$K_{O_2}$ (atm <sup>-1</sup> )	Reference
4-CP	Degussa P25 TiO <sub>2</sub>	10.5	[38]
4-CP <sup>a</sup>	Degussa P25 TiO <sub>2</sub>	4.4	[11]
Phenol	TiO <sub>2</sub> from Wako Chem. Co.	11.1	[28]
Methyl orange	Anatase TiO <sub>2</sub> from Merck Co.	4.2	[10]
4-CP	Degussa P25 TiO <sub>2</sub>	17.6	This work
4-NP	Degussa P25 TiO <sub>2</sub>	9.98	This work
Phenol	Degussa P 25 TiO <sub>2</sub>	12.7	This work

<sup>a</sup> Based on the formation rate of CO<sub>2</sub>.

Henry's Law can be applied to these gases, the variations in the ratio of O<sub>2</sub>/N<sub>2</sub> have the effect of varying both the gas phase partial pressure of oxygen and the dissolved oxygen concentration in the aqueous phase. It should be noted that photocatalytic degradation of organic compounds was almost quenched in the absence of dissolved oxygen (purged with pure N<sub>2</sub>). Although hydroquinone (HQ) was identified as the intermediate of 4-CP, its concentration was very low (less than 1 ppm) even after 1 h illumination. Above finding suggests that transformation of 4-CP to HQ was very slow in the absence of O<sub>2</sub>, and therefore negligible. The influence of dissolved oxygen on the observed degradation kinetic constant can be well described by Eq. (8).

$$k_{\text{obs}} = \frac{kK_{O_2}p_{O_2}}{1 + K_{O_2}p_{O_2}} \quad (8)$$

$K_{O_2}$  is considered as adsorption constant of dissolved oxygen on TiO<sub>2</sub> catalyst, but  $k$  value has no absolute meaning because it depends on the experimental conditions. The  $K_{O_2}$  values experimentally obtained in this study are comparable with those reported in literature, which are listed in Table 3.

### 3.4. Adsorptive characteristics on P25 TiO<sub>2</sub>

The key steps of the photocatalytic degradation are the reactions between adsorbed species. Consequently, the photocatalytic process strongly depends on the adsorptive properties of the organic compounds. In this study, the adsorption experiments of phenol, 4-CP and 4-NP have been investigated in TiO<sub>2</sub> suspensions at natural pH value and room temperature. Results demonstrated that Langmuir model could well describe the adsorption processes of above three com-

pounds and the adsorptive parameters are listed in Table 4. Although the  $K_s$  in Eq. (7) is generally taken as the equilibrium adsorptive constants of organics on TiO<sub>2</sub>, but, the results clearly show that the adsorption constants obtained from the kinetic experiments are different from those obtained from the dark adsorption experiments for the three model compounds (Table 2: Column 6, Table 4: Column 3).

Assuming that a complete monolayer of organic compound is formed on the surface of TiO<sub>2</sub>, the maximum surface coverage based on  $Q_{\text{max}}$  for the above compounds can be calculated by the following equation and are listed in Column 4 of Table 4.

$$\theta_{\text{max}} = \frac{Q_{\text{max}}N_A\sigma_0}{A_{\text{SP}}} \times 100\% \quad (9)$$

where  $Q_{\text{max}}$  is maximum adsorption capacity of pollutant over catalyst (mol/g),  $N_A$  the Avogadro's number,  $\sigma_0$  the average cross-sectional area of organic molecule [39] and  $A_{\text{SP}}$  the specific surface area of the catalyst (50 m<sup>2</sup>/g). As the maximum surface coverages for these three compounds are extremely low, it indicates that most of the potential sites of the catalyst are not accessible to these species. This may result from the presence of high concentration of H<sub>2</sub>O and/or OH<sup>-</sup> on the surface of TiO<sub>2</sub>. It is well known that the surface of TiO<sub>2</sub> is readily hydroxylated when it is in contact with water. Both dissociated and molecular water are bonded to the surface of TiO<sub>2</sub>. Surface coverages of 7–10 OH<sup>-</sup> nm<sup>-2</sup> at room temperature were reported in literature [40]. Under the experimental conditions where the concentration of organics is around 0.2 mM, the surface coverages are even much lower (Table 4, Column 5). The reaction between hydroxyl radical and adsorbed organics is the main step of the photocatalytic process, and the degradation rate is proportional to the surface coverage. Therefore, one

Table 4  
Adsorptive and mass transfer parameters

Pollutant	$Q_{\max}$ ( $\mu\text{mol/g}$ )	$K_s$ ( $\text{mM}^{-1}$ )	$\theta_{\max}$ (%)	$\theta$ (%)	$(C_s/C_b)_{\min}$	$\eta_{\min}$
4-NP	5.94	1.06	1.7	0.30	0.990	0.910
4-CP	4.20	2.83	1.2	0.45	0.989	0.906
Phenol	3.28	0.82	0.95	0.14	0.989	0.902
Oxygen					0.992	

of the main reasons that result in the low efficiency of the photocatalytic process is the extremely low surface coverage of organics on  $\text{TiO}_2$  catalyst.

### 3.5. Mass transfer in photocatalytic reactions

$\text{P25 TiO}_2$  is a non-porous catalyst and its external mass transfer rate can be determined by the following equation:

$$r_m = 10^3 k_m (C_b - C_s) A'_{\text{SP}} W \quad (\text{mmol/l/s}) \quad (10)$$

where the factor  $10^3$  is required to render the units consistent in the equation,  $C_b$  and  $C_s$  are the bulk and local concentration ( $\text{mM}$ ) of organics, respectively,  $W$  is the catalyst dosage ( $\text{g l}^{-1}$ ),  $A'_{\text{SP}}$  is the modified specific surface area of the catalyst. Modified surface area is used because catalyst particle in aqueous solution was reported [41] to be up to  $5 \mu\text{m}$  in diameter due to the aggregation of the elementary particles. Mass transfer coefficient for a spherical particle in stirred solution can be estimated by the following equation [42]:

$$Sh = \frac{2Rk_m}{D} = 2 + 0.6Re_p^{1/2} Sc^{1/3} \quad (11)$$

where  $D$  is the diffusivity of organics in water,  $R$  the actual radius of catalyst particle,  $Re_p$  the Reynold's number of solid particle, and  $Sc$  the Schmidt number. For estimation,  $k_m$  takes its lowest value ( $k_m = D/R$  when the particle is stationary) in this study. Assuming that at steady state the mass transfer rate is equal to the photodegradation rate determined by the kinetic experiments, then, the minimum value of the ratio of  $C_s$  to  $C_b$  can be calculated for all organics and oxygen and are listed in Table 4. The results indicate that the mass transfer resistance of organics and oxygen in  $\text{TiO}_2$  suspensions can definitely be neglected as  $C_b$  is almost equal to  $C_s$ .

As mentioned earlier,  $\text{P25 TiO}_2$  is non-porous and its elementary particle size is around  $0.03 \mu\text{m}$ . However, it has been reported [41] that in aqueous suspensions the actual catalyst particles become much bigger and may be up to  $5 \mu\text{m}$  in diameter due to aggregation. In this case, the effect of the intra-particle pore diffusion can be evaluated by the magnitude of the Thiele modulus,  $\phi_s$ , which was defined in [43]:

$$\phi_s = R \sqrt{\frac{k_v C_s^{n-1}}{D_e}} \quad (12)$$

For first order reaction, Eq. (12) can be reduced to:

$$\phi_s = R \sqrt{\frac{k_v}{D_e}} \quad (13)$$

where  $k_v$  is the apparent rate constant based on the volume of catalyst, and  $D_e$  the effective diffusivity of organics within the  $\text{TiO}_2$  aggregates. The  $k_v$  values for phenol, 4-CP and 4-NP were determined by the kinetic experiments. The effective diffusivity  $D_e$  takes its lowest value of  $10^{-12} \text{m}^2/\text{s}$ , which is of the same order of magnitude as the diffusion coefficient in porous solids. On the basis of these data, the Thiele modulus was calculated, and subsequently the effectiveness factor ( $\eta$ ) of the  $\text{TiO}_2$  aggregates was estimated from the following equation [43] and are listed in Column 7 of Table 4:

$$\eta = \frac{3}{\phi_s} \left( \frac{1}{\tan h \phi_s} - \frac{1}{\phi_s} \right) \quad (14)$$

The results indicate that the minimum effectiveness factors for all the compounds investigated are above 0.9. Consequently, the internal mass transfer resistance in the  $\text{TiO}_2$  aggregates can be neglected, and the chemical reaction is the rate-determining step in the photocatalytic process of phenol, 4-CP and 4-NP in  $\text{TiO}_2$  suspensions.

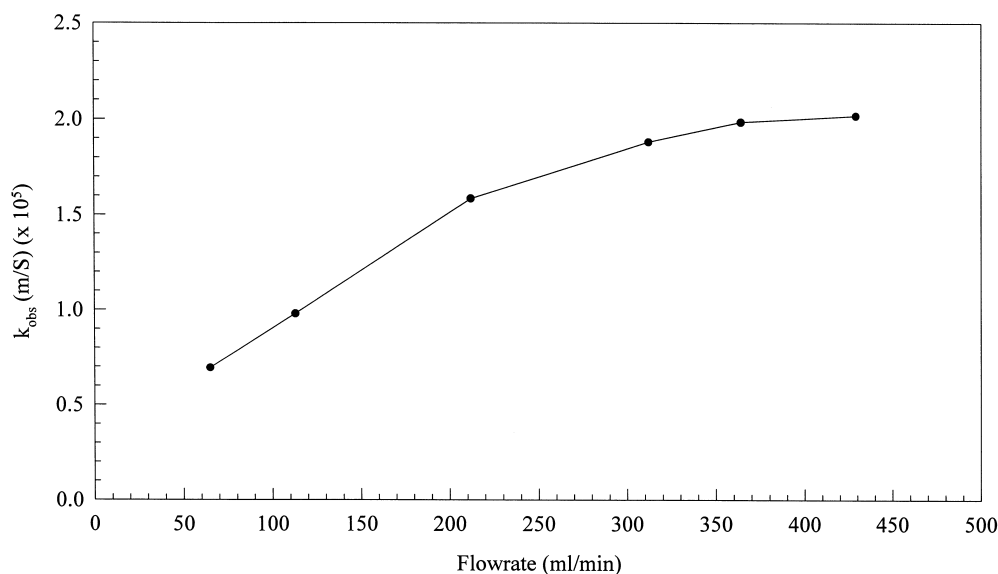


Fig. 6. Influence of circulating flow rate on the degradation of 4-NP in TiO<sub>2</sub> immobilized system. (Experimental conditions:  $I = 16.2 \text{ mW/cm}^2$ ;  $C_0 = 0.10 \text{ mM}$ ;  $T = 303 \text{ K}$ ,  $(\text{TiO}_2) = 0.473 \text{ mg/cm}^2$ ; O<sub>2</sub> saturated; pH natural).

However, mass transfer limitation occurred in TiO<sub>2</sub> immobilised system [44]. Fig. 6 shows the influence of circulating flowrate on the degradation rate constant of 4-NP and reveals that external mass transfer plays a significant role for low flow rate. The results show that decomposition rate increases with increasing flow rate and reaches a plateau at a flow rate of about 400 ml/min. The effect can be described by the following relationship:

$$k_{obs} = \frac{a\omega F}{1 + \omega F} \quad (15)$$

with the proportionality constant  $\omega$  value of 4.1 min/l. Similar results have also been reported by Matthews [6].

### 3.6. Calcination temperature

For TiO<sub>2</sub> immobilized system, another factor that affects the activity of the catalyst must be investigated is the catalyst preparation method. Before the coated catalyst is used in the photocatalytic experiments, it must be calcined at a high temperature. Otherwise, the catalyst film will not have enough mechanical strength. The calcination temperature influences the catalyst activity because it affects the physical properties of the

catalyst such as porosity, surface area, crystal structure, crystal size, as well as the mechanical strength of the catalyst film. In this study, six glass plates coated with almost the same amount of catalyst were calcined at different temperature (423–873 K) for 3 h. Fig. 7 represents the effect of calcination temperature on the photocatalytic activities of the TiO<sub>2</sub> catalyst. The apparent reaction rate, defined as per unit weight of catalyst, decreased as the annealing temperature increased. For comparison, influence of calcination temperature on the adsorption property and reactivity of the original powdered P25 catalyst was also investigated. Fig. 8 illustrates the dynamic physical adsorption of salicylic acid on powdered TiO<sub>2</sub> calcined at different temperatures. We selected salicylic acid as model compound as it has much higher adsorption capacity than 4-NP, which increases accuracy of experimental results. The adsorption data in Fig. 8 were analyzed using following expression:

$$Q = Q_e [1 - \exp(-k_{ads}t)] \quad (16)$$

where  $Q$  and  $Q_e$  are, respectively, the adsorption capacities at time  $t$  and at equilibrium,  $k_{ads}$  is the adsorption rate constant.  $k_{ads}$  values of catalysts calcined at different temperatures was obtained using the

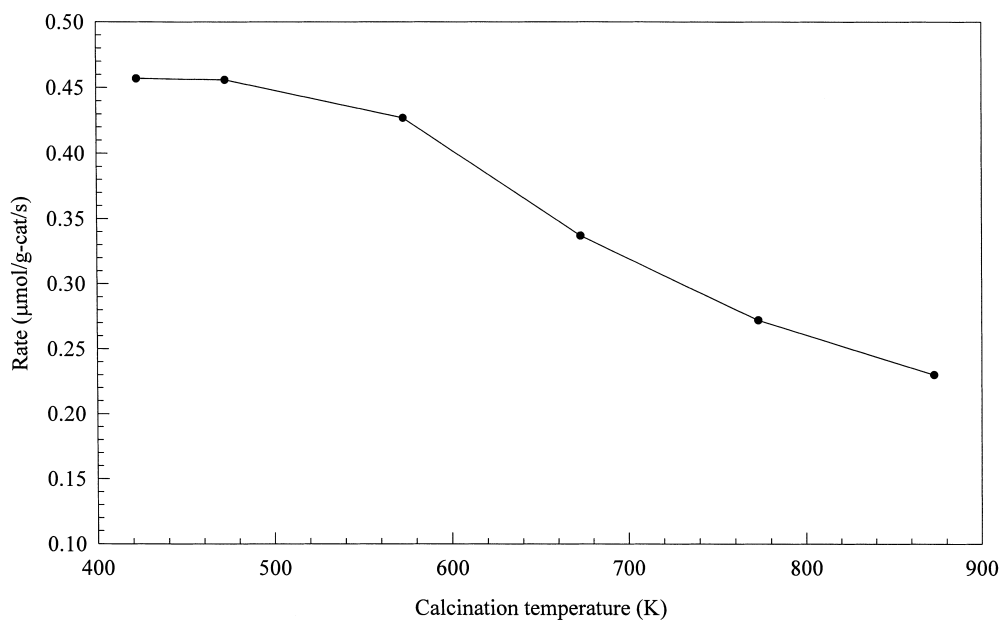


Fig. 7. Influence of calcination temperature on the degradation of 4-NP in  $\text{TiO}_2$  immobilized system. (Experimental conditions:  $I = 15.9 \text{ mW/cm}^2$ ;  $C_0 = 0.10 \text{ mM}$ ,  $T = 303 \text{ K}$ ;  $(\text{TiO}_2) = 0.47\text{--}0.51 \text{ mg/cm}^2$ ;  $Q = 425 \text{ ml/min}$ ;  $\text{O}_2$  saturated; pH natural).

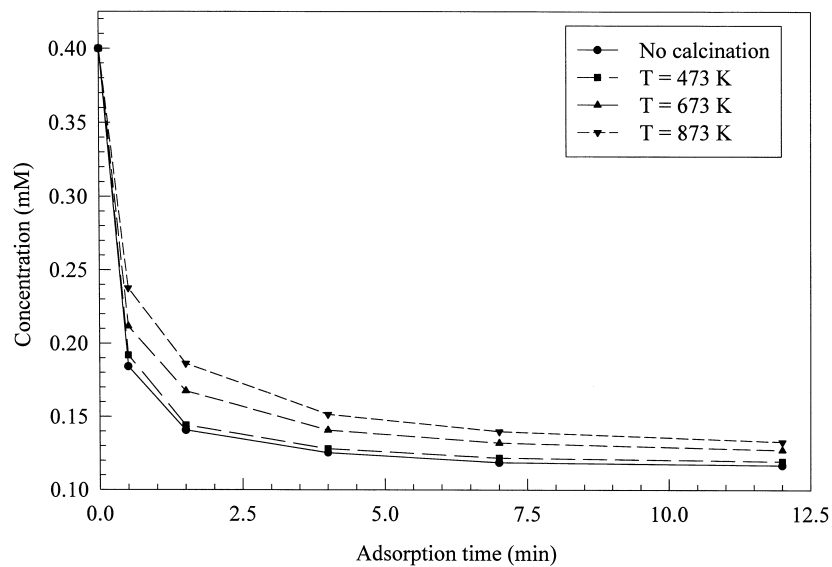


Fig. 8. Dynamic physical adsorption of salicylic acid over powdered P25  $\text{TiO}_2$  calcined at different temperatures.  $(\text{TiO}_2) = 8 \text{ g/l}$ .

linear interpolation based on Eq. (17) and are listed in Table 5.

$$\ln(Q_e - Q) = \ln Q_e - k_{\text{ads}} t \quad (17)$$

The result indicates that adsorption rate constant decreased with the increase of the calcination temperature. Mills and Morris [45] reported that no loss in catalyst surface area was observed when powdered

Table 5  
Influence of calcination temperature on  $k_{\text{ads}}$  over powdered  $\text{TiO}_2$

$T$ (K)	$k_{\text{ads}}$ ( $\text{min}^{-1}$ )
No calcinating	0.454
473	0.448
673	0.371
873	0.311

$\text{P25 TiO}_2$  was calcinated at temperature lower than  $600^\circ\text{C}$ , while phase transition, from anatase to rutile, occurred at temperature above  $600^\circ\text{C}$ . Hence, it appears that the decrease of adsorption rate constant results primarily from the reduction of catalyst's affinity to organic compound. However, photocatalytic degradation experiments over powdered catalyst in five different calcination temperatures from  $200$  to  $600^\circ\text{C}$  demonstrated that catalyst activity change was within experimental errors. It suggests that the reactivity of the photocatalyst was not influenced by the calcination temperature and dynamic physical adsorption of the organic compound was not the rate determining step. Therefore, in this study the decrease of reactivity of the immobilized catalyst film mainly resulted from the increase of internal mass transfer resistance with the annealing temperature. It is likely that during the heating process a part of porous structure gets lost through sintering process, especially for films composed of nanoparticles, and the catalyst film becomes denser at higher temperature, which has adverse effect on the mass transfer for organic species. Another possibility [46] is that higher calcination temperature might result in the migration of some cations, such as  $\text{Na}^+$  and  $\text{Si}^{4+}$ , from the glass into the catalyst layer, which may increase the recombination of photo-generated electrons and holes. Therefore, high calcination temperature did not favour the catalyst activity. Although, the catalyst calcined at low temperature had high activity, in this study considerable loss of catalyst ( $T_c < 473$  K) was observed, particularly at high circulating flowrate of solution. Thus, the optimal calcination temperature observed was around  $573$  K.

#### 4. Conclusions

Heterogeneous photocatalysis has been extensively investigated as a promising candidate for water

purification. Catalyst dosage is one of the important kinetic factors and Eq. (3) can well predict the optimal catalyst dosage for different photo-systems. Other operational parameters have also been carefully studied and their influences on the photocatalytic degradation can be correlated by Eq. (7) for 4-CP, 4-NP, and phenol in  $\text{P25 TiO}_2$  suspensions. The kinetic parameters in Eq. (7) have been experimentally determined. The low efficiency of the photocatalytic process may result from the extreme low surface coverage of organics on the catalyst. Both the external and internal mass transfer resistances are negligible for the photocatalytic process in aqueous  $\text{TiO}_2$  suspensions. However, for catalyst immobilized system, mass transfer resistance plays a significant role at lower circulating flowrate and there also exists an optimal catalyst dosage or thickness of the catalyst film. Calcination temperature had no effect on the activity of the powdered  $\text{P25 TiO}_2$  catalyst, but activity loss was observed in immobilized  $\text{P25 TiO}_2$  calcined at high temperature. The ideal calcination temperature observed for immobilized  $\text{TiO}_2$  was around  $573$  K.

#### Acknowledgements

The authors gratefully acknowledge the funding of the project by the National University of Singapore (RP960629) and the award of a research scholarship to Dingwang Chen.

#### References

- [1] M.R. Hoffmann, S.T. Martin, W. Choi, D.W. Bahnemann, *Chem. Rev.* 95 (1995) 69.
- [2] D.F. Ollis, H. Al-Ekabi (Eds.), *Photocatalytic Purification and Treatment of Water and Air*, Elsevier, Amsterdam, 1993.
- [3] N. Serpone, E. Pelizzetti (Eds.), *Photocatalysis, Fundamentals and Applications*, Wiley, New York, 1989.
- [4] R.W. Matthews, *J. Chem. Soc. Faraday Trans. I* 80 (1984) 457.
- [5] R.W. Matthews, *Wat. Res.* 24 (1990) 653.
- [6] R.W. Matthews, *J. Phys. Chem.* 91 (1987) 3328.
- [7] R.W. Matthews, *J. Catal.* 111 (1988) 264.
- [8] A.L. Pruden, D.F. Ollis, *J. Catal.* 82 (1983) 404.
- [9] E. Pelizzetti, C. Minero, V. Maurino, A. Scalfani, H. Hidaka, N. Serpone, *Environ. Sci. Technol.* 23 (1989) 1380.
- [10] L.C. Chen, T.C. Chou, *Ind. Eng. Chem. Res.* 32 (1993) 1520.
- [11] A. Mills, S. Morris, *J. Photochem. Photobiol. A: Chem.* 71 (1993) 75.

- [12] Y. Inel, A. Okte, J. Photochem. Photobiol. A: Chem. 96 (1996) 175.
- [13] M.C. Lu, G.D. Roam, J.N. Chen, C.P. Huang, J. Photochem. Photobiol. A: Chem. 76 (1993) 103.
- [14] H.Y. Chen, O. Zahraa, M. Bouchy, F. Thomas, J.Y. Bottero, J. Photochem. Photobiol. A: Chem. 85 (1995) 179.
- [15] J. Cunningham, G. Al-Sayyed, J. Chem. Soc., Faraday Trans. 86 (1990) 3935.
- [16] A.K. Ray, A.A.C.M. Beenackers, *AIChE J.* 47 (1997) 2571.
- [17] H. Al-Ekabi, N. Serpone, E. Pelizzetti, C. Minero, M.A. Fox, R.B. Draper, *Langmuir* 5 (1989) 250.
- [18] M.S. Dieckmann, K.A. Gray, *Wat. Res.* 30 (1996) 1169.
- [19] Y. Ku, R.M. Leu, K.C. Lee, *Wat. Res.* 30 (1996) 2569.
- [20] G. Al-Sayyed, J.C. D'Oliveira, P. Pichat, J. Photochem. Photobiol. A: Chem. 58 (1991) 99.
- [21] J.P. Percherancier, R. Chapelon, B. Pouyet, J. Photochem. Photobiol. A: Chem. 87 (1995) 261.
- [22] J.C. D'Oliveira, G. Al-Sayyed, P. Pichat, *Environ. Sci. Technol.* 24 (1990) 990.
- [23] V. Augugliaro, L. Palmisano, M. Schiavello, A. Sclafani, L. Marchese, G. Martra, F. Miano, *Appl. Catal.* 69 (1991) 323.
- [24] S. Lakshmi, R. Renganathan, S. Fujita, J. Photochem. Photobiol. A: Chem. 88 (1995) 163.
- [25] R. Terzian, N. Serpone, J. Photochem. Photobiol. A: Chem. 89 (1995) 163.
- [26] V. Augugliaro, V. Loddo, G. Marci, L. Palmisano, M.J. Lopez-Munoz, *J. Catal.* 166 (1997) 272.
- [27] D.W. Chen, A.K. Ray, *Wat. Res.* 32 (1998) 3223.
- [28] K. Okamoto, Y. Yamamoto, H. Tanaka, A. Itaya, *Bull. Chem. Soc. Jpn.* 58 (1985) 2023.
- [29] J.C. Crittenden, J.B.D.L. Perram, J.B. Liu, D.W. Hand, *Wat. Res.* 31 (1997) 429.
- [30] D.W. Chen, F.M. Li, A.K. Ray, *Wat. Res.*, submitted for publication.
- [31] C. Minero, F. Catozzo, E. Pelizzetti, *Langmuir* 8 (1992) 481.
- [32] H. Gerischer, A. Heller, *J. Phys. Chem.* 95 (1991) 5261.
- [33] C.M. Wang, A. Heller, H. Gerischer, *J. Am. Chem. Soc.* 114 (1992) 5230.
- [34] R.M. Alberici, W.F. Jardim, *Wat. Res.* 28 (1994) 1845.
- [35] J. Sabate, M.A. Anderson, H. Kikkawa, M. Edwards, C.G. Hill, *J. Catal.* 127 (1991) 167.
- [36] C.Y. Hsiao, C.L. Lee, D.F. Ollis, *J. Catal.* 82 (1983) 418.
- [37] A. Sclafani, L. Palmisano, E. Davi, *New J. Chem.* 14 (1990) 265.
- [38] A. Mills, R. Davies, J. Photochem. Photobiol. A: Chem. 85 (1995) 173.
- [39] J.O. Hirschfelder, C.F. Curtiss, R.B. Bird, *Molecular Theory of Gases and Liquids*, Wiley, New York, 1954.
- [40] Y. Suda, T. Morimoto, *Langmuir* 3 (1987) 786.
- [41] H.Y. Chen, O. Zahraa, M. Bouchy, F. Thomas, J.Y. Bottero, J. Photochem. Photobiol. A: Chem. 85 (1995) 179.
- [42] Y.T. Shaw, *Gas-Liquid-Solid Reactor Designs*, McGraw-Hill, New York, 1979.
- [43] O. Levenspiel, *Chemical Reaction Engineering*, 2nd ed., Wiley, New York, 1972.
- [44] C.S. Turchi, D.F. Ollis, *J. Phys. Chem.* 92 (1988) 6853–6854.
- [45] A. Mills, S. Morris, J. Photochem. Photobiol. A: Chem. 71 (1993) 285.
- [46] A. Fernandez, G. Lassaletta, V.M. Jimenez, *Appl. Catal. B: Environmental* 7 (1995) 49.